Dynamic surface tension of surfactant TA: experiments and theory

D. R. OTIS, JR., E. P. INGENITO, R. D. KAMM, AND M. JOHNSON
Department of Mechanical Engineering, Massachusetts Institute of Technology, Cambridge 02139; and Division of Pulmonary and Critical Care Medicine, Department of Medicine, Brigham and Women's Hospital, Boston, Massachusetts 02115

Otis, D. R., Jr., E. P. Ingenito, R. D. Kamm, and M. Johnson. Dynamic surface tension of surfactant TA: experiments and theory. *J. Appl. Physiol.* 77(6): 2681–2688, 1994.—A bubble surfactometer was used to measure the surface tension of an aqueous suspension of surfactant TA as a function of bubble area over a range of cycling rates and surfactant bulk concentrations. Results of the surface tension-interfacial area loops exhibited a rich variety of phenomena, the character of which varied systematically with frequency and bulk concentration. A model was developed to interpret and explain these data and for use in describing the dynamics of surface layers under more general circumstances. Surfactant was modeled as a single component with surface tension taken to depend on only the interfacial surfactant concentration. Two distinct mechanisms were considered for the exchange of surfactant between the bulk phase and interface. The first is described by a simple kinetic relationship for adsorption and desorption that pertains only when the interfacial concentration is below its maximum equilibrium value. The second mechanism is "squeeze-out" by which surfactant molecules are expelled from an interface compressed past a maximum packing state. The model provided good agreement with experimental measurements for cycling rates from 1 to 100 cycles/min and for bulk concentrations between 0.0073 and 7.3 mg/ml.

pulmonary surfactant; modeling; isotherm; Langmuir; squeeze-out

BY THEIR NATURE, surfactants in suspension migrate to an interface where they reduce the free energy of the surfactant-solvent system and the surface tension of the interface. If the interface is perturbed from an equilibrium state the surfactant concentration and surface tension of the interface may change, and subsequent exchange of surfactant between the interface and the bulk suspension minimizes the free energy of the system.

The air spaces of the lung are coated by a thin film or liquid layer containing pulmonary surfactant composed of phospholipids (~90%) and various proteins (10%) that are secreted by type II epithelial cells lining the alveolar walls (21). During breathing, this film periodically expands and contracts, resulting in a periodic variation in interfacial surfactant concentration and thereby surface tension. This variation in surface tension with lung volume stabilizes alveoli at low lung volumes and reduces the work of breathing (29). The hysteresis evident in the surface tension-lung volume loops is a major contributor to the hysteresis in lung pressure-volume curves during total lung capacity maneuvers (26).

To measure how surface tension varies as a function of pulmonary surfactant interfacial concentration, various instruments have been used to examine surfactant material from excised lungs in vitro. Among these are the Langmuir trough used with a Wilhelmy balance (15), the captive bubble apparatus (22), and the bubble surfactometer (5). This last instrument consists of a chamber of liquid in which a nearly spherical bubble is formed at the end of a narrow tube and then the bubble volume is cycled sinusoidally with time. Knowledge of the bubble volume and the pressure difference across the bubble allows one to calculate the dynamic surface tension through the Laplace law. The bubble surfactometer has been employed extensively in studies of the dynamic characteristics of pulmonary surfactants.

An analytic study was undertaken by Horn and Davis (11) to consider how hysteresis evident in surface tension-surface area (γ-A) loops for oscillating bubbles might be caused by *1*) diffusion of surfactant between bulk and interface, *2*) adsorption between bulk and interface, *3*) viscoelastic behavior in the interface, and *4*) viscoelastic behavior in the bulk. They concluded that hysteresis is due largely to viscoelasticity of the interface. However, although both diffusion and adsorption were considered as transfer mechanisms, no provision was made for "squeeze-out" phenomena or monolayer collapse at high interfacial concentrations (7). Moreover, these investigators did not allow for the variation of kinetic processes with interfacial concentration (26).

Other than the study of Horn and Davis (11), there has been no attempt to create a comprehensive model to explain the change in surface tension that occurs as lung surfactant or its analogues are cycled dynamically through area changes by the devices discussed above. Surfactant TA [Tokyo Tanabe, Tokyo (also known as Survanta, Ross Laboratories, Columbus, OH)] is a semisynthetic preparation widely used clinically to treat respiratory distress syndrome (RDS). We used a bubble surfactometer to determine how surface tension of films of surfactant TA varies as the film area is cycled at various rates and bulk concentrations. A model was then developed to compare with the data generated, emphasizing the kinetic aspects of the process. This model allowed us to understand in greater detail the physicochemical behavior of surfactant TA in air-liquid interfaces and raised new questions that need to be addressed by further experiments.

MATERIALS AND METHODS

Surfactant TA was received as a suspension in normal saline (25 mg/ml; Ross Laboratories). Before each experiment, a fresh suspension was prepared by diluting the surfactant with 5 mM $CaCl_2$ (19) to concentrations between 0.0073 and 7.3 mg/ml; all of these experiments were conducted with surfactant from a single lot. The suspension was carefully vortexed and sonicated on ice three times for 30 s (avoiding the formation of any foam on the surface).

A small set of experiments was conducted to ascertain whether dilution of the surfactant in saline (with 5 mM $CaCl_2$) would give different results than with 5 mM $CaCl_2$ alone. These were performed with a separate lot of surfactant TA but prepared in all other respects similarly.

0161-7567/94 $3.00 Copyright © 1994 the American Physiological Society

Bubble surfactometer. The γ-A measurements were made using a pulsating bubble surfactometer (Electronetics, Amherst, NY). A small spherical bubble of air was formed at the lower end of a 0.4-mm capillary in a suspension containing the surfactant, and the bubble volume was then cycled so that the air-liquid interface area changed with time. Measurement of the bubble radius and the pressure difference across the bubble allows one to calculate the dynamic surface tension through the Laplace law. The variations in bubble volume are equal to the known piston displacement, and the initial bubble volume is measured through calibrated optics. The mean bubble diameter is on the order of 1 mm and remains nearly spherical for surface tension values down to a few dynes per centimeter (8, 25).

The system was modified to allow access to the analog signals for pressure within the bubble and minimum radius as functions of time. These data were processed using data collection and analysis software (Labtech Notebook, Taunton, MA), an analog-to-digital converter (12-bit Dash-8, Metrabyte, Taunton, MA), and a personal computer (Compu-Add 8086 PC, Austin, TX). Calibrations of both the surfactometer and the computerized data collection system were performed daily using doubly distilled water. Static and dynamic controls with distilled water were carried out both before and after measurements. All experiments were conducted at 37°C.

Measurements of the equilibrium surface tension at bulk concentrations of 0.0073, 0.073, and 0.73 mg/ml were made by forming a bubble of radius 0.4 mm, holding it constant at that size, and then measuring surface tension as a function of time until it reached a constant value.

Dynamic γ-A measurements were conducted at cycling rates ranging from 1 to 100 cycles/min, varying the bubble radius from a minimum of 0.4 mm to a maximum (fixed for a particular experiment) of 0.53–0.59 mm. Analog transfilm pressure and radius signals were sampled at 100 Hz. Results represent stable stationary-state values (25), which are defined as when the shape of the γ-A loops no longer changed from one cycle to the next; this state typically took ~30 min to achieve. Once a stationary condition was reached, the variability in the γ-A relationship from one loop to the next was small (usually <10%). The repeatability of the loops from one sample preparation to another showed greater variability with the hysteretic area of the γ-A loop showing as much as a 33% variation and the minimum surface tension varying by as much as 5 dyn/cm; however, the overall pattern (see Fig. 4, *A–D*) was always apparent.

Theoretical model. We assumed transport of the surfactant to the surface to be an adsorption-limited as opposed to a diffusion-limited process (see DISCUSSION). As such, the bulk suspension was considered to be well mixed at all times at a bulk concentration of C. The kinetics of adsorption and desorption were defined by three interfacial surfactant concentration (Γ) regimes (Fig. 1): *1)* Γ less than the maximum equilibrium Γ^* [the limiting value of Γ reached as C is increased (γ^* is γ of the film when $\Gamma = \Gamma^*$)], *2)* Γ greater than this concentration but less than Γ_{max} (the maximum dynamic concentration of surfactant obtainable on dynamic compression of the interface) and *3)* $\Gamma = \Gamma_{max}$, (γ_{min} is γ of the film when $\Gamma = \Gamma_{max}$).

For the first regime with $\Gamma < \Gamma^*$, adsorption to the bubble surface is assumed to follow Langmuir kinetics (1, 11)

$$\frac{dM}{dt} = A[k_1C(\Gamma^* - \Gamma) - k_2\Gamma] \qquad (1)$$

where t is time (in min), k_1 is the adsorption coefficient (in $cm^3 \cdot g^{-1} \cdot min^{-1}$), k_2 is the desorption coefficient (in min^{-1}), A is the surface area of the bubble (in cm^2), and M (which equals ΓA) is the amount of surfactant in the interface (in g). Note that *Eq. 1* predicts adsorption for interfacial concentration less than the equilibrium concentration (Γ_{eq}) (between *points G* and *B* on loop in Fig. 1) and desorption for concentrations greater than this (*segments BC* and *FG*)

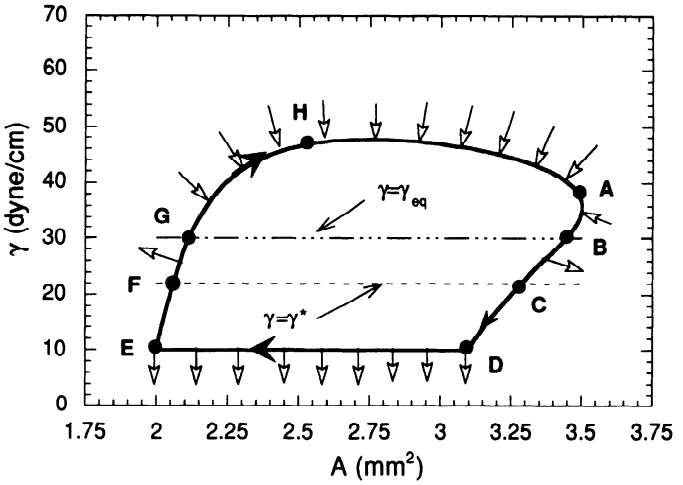

FIG. 1. Schematic of surface tension (γ)-bubble surface area (A) loop demonstrating surfactant transfer mechanisms for each loop segment: kinetic adsorption (*segment GB*) or desorption (*segments BC* and *FG*) for $\gamma > \gamma^*$ [where γ^* is γ at maximum equilibrium surface concentration (Γ^*)] (1st regime), insoluble monolayer for $\gamma_{min} < \gamma < \gamma^*$ [where γ_{min} is γ at maximum dynamic surface concentration (Γ_{max})] (*segments CD* and *EF*; 2nd regime), and squeeze-out as area is lowered beyond point where γ_{min} is reached (*segment DE*; 3rd regime). Inward and outward arrows represent, adsorption, desorption, or squeeze-out of surfactant from monolayer.

$$\frac{\Gamma_{eq}}{\Gamma^*} = \frac{k_1C}{k_1C + k_2} \qquad (2)$$

where Γ_{eq} is the interfacial concentration of surfactant that is in equilibrium with a given C (γ_{eq} is γ of the film when $\Gamma = \Gamma_{eq}$). As $C \rightarrow \infty$, $\Gamma_{eq} \rightarrow \Gamma^*$ (the maximum equilibrium interfacial concentration of surfactant).

Inherent in Langmuir kinetics is the assumption that the interface consists of a given number of adsorption sites (defined by Γ^*) and that the adsorbed species interact with each site without any cooperativity. Γ^* corresponds to a minimum equilibrium γ (22.2 dyn/cm) determined by equilibrium measurements using the bubble surfactometer in the limit as C is increased.

In the second regime with $\Gamma^* < \Gamma < \Gamma_{max}$, the monolayer is modeled as insoluble; i.e., it does not exchange surfactant material with the subphase. In this regime, Γ can change only because of changes in A; as A decreases, the concentration rises

$$\Gamma = \Gamma^* \frac{A^*}{A} \qquad (3)$$

up to a maximum value of $\Gamma = \Gamma_{max}$.

In the third regime, when Γ reaches Γ_{max}, the surfactant molecules are packed as tightly as possible in the interface and Γ can rise no higher. γ reaches its minimum value here, and any further compression is taken to result in a loss (or squeezing out) of surfactant material into the bulk phase (7). These regimes have previously been described for dipalmitoylphosphatidylcholine and lung surfactant extract by Tchoreloff et al. (28) to be the liquid-expanded ($\Gamma < \Gamma^*$), liquid-condensed ($\Gamma^* < \Gamma < \Gamma_{max}$), and solid ($\Gamma = \Gamma_{max}$) (or collapsed monolayer) states.

As in the bubble surfactometer, the volume of the bubble (V) is modeled varying as

$$V = V_{mean} + \Delta V \sin(2\pi\omega t + \pi/2) \qquad (4)$$

where V_{mean} is the mean bubble volume, ΔV is the amplitude of the cyclic variation, and ω is the oscillation frequency. A is then determined from the volume with the assumption of a spherical shape. Numerical simulation begins at $t = 0$ with V = maximum $V = (V_{mean} + \Delta V)$ and an initial number of moles (N_0) of surfactant at the interface such that the initial interfacial concentra-

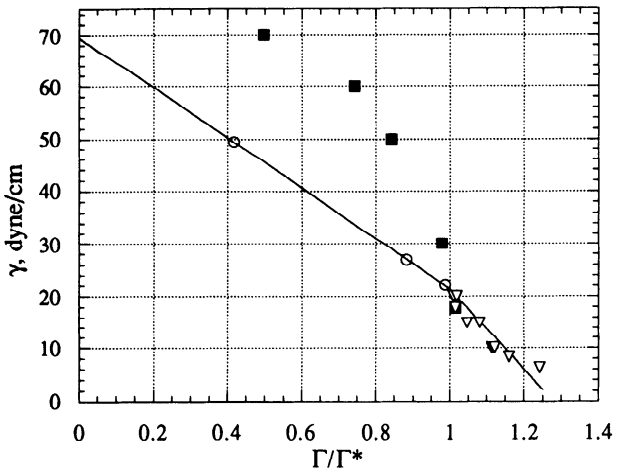

FIG. 2. Isotherm relating γ to surface concentration (Γ) of surfactant for single-component surfactant used in model. ○, $\Gamma < \Gamma^*$ (determined from *Eq. 2* and equilibrium data shown in Fig. 3); ▽, $\Gamma^* < \Gamma < \Gamma_{max}$ (determined from deflation phase of high-frequency dynamic loops using *Eq. 3*); solid line, best fit to this data determined by matching slopes at low Γ ($\Gamma < \Gamma^*$) and high Γ ($\Gamma > \Gamma^*$) and requiring these 2 lines to meet at $\Gamma = \Gamma^*$ at minimum equilibrium surface tension. Also shown is 2nd isotherm (■) found using data from inflation phase (*segment EH* of Fig. 1) of 1 of high-frequency loops (0.073 mg/ml, 100 cycles/min), determined by again assuming surfactant to be insoluble and using *Eq. 3*. $\gamma(\Gamma_{max}) = \gamma_{min} = 10$ dyn/cm; $\gamma(\Gamma^*) = \gamma^* = 22.2$ dyn/cm.

tion is N_0/(maximum A); on cycling, surfactant transport to or from the interface is defined by the three regimes described above. The results were not affected by the value chosen for N_0, since the calculation was continued until a stationary condition was reached.

Time stepping was performed using a third-order Adams-Bashforth technique. At each time step, the value of Γ/Γ^* was determined: the form of the equations allowed us to determine this ratio without ever determining an absolute value of Γ. Thus, we did not determine Γ^*. Because of the symmetry of the bubble, we took Γ and hence γ to be uniform over its entire surface, noting, however, that the presence of the needle would introduce some artifact in the experiment not mimicked in the model.

Isotherm used to find γ. Once the interfacial surfactant concentration (Γ/Γ^*) as a function of time is obtained, γ is taken to be a function of Γ as

$$\gamma = \gamma^* f(\Gamma/\Gamma^*) \qquad (5)$$

The isotherm f (Fig. 2) is found in two steps. For $\Gamma < \Gamma^*$, *Eq. 1* can be solved at steady state, yielding *Eq. 2*. Because the equilibrium γ is known as a function of C, the isotherm can be determined once k_1 and k_2 are determined from the dynamic data. For $\Gamma^* < \Gamma < \Gamma_{max}$ (2nd regime), pooled data from the dynamic experiments with a frequency of 100 min^{-1} (the highest frequency tested) are used: because the surfactant is assumed insoluble in this regime, *Eq. 3* is used to calculate Γ as a function of A during the deflation phase of the cycle (*segment CD*).

Using the isotherm, model computations were then performed to explore the k_1-k_2 parameter space, and the k_1 and k_2 values that best matched the experimental data were determined. In practice, it was found that the model predictions were insensitive to the value of k_2 at higher C and thus k_1 was determined from the higher C data (0.073–7.3 mg/ml) by visually picking the best match to the shape of the loops. To find the best value for k_2, the data at a low C (0.0073 mg/ml) were used, finding the ratio of k_1C to k_2, which gave the best match to the lowest γ measured on these loops. In practice, k_1 and k_2 were varied until changes in their values yielded changes in the shape of the γ-A loops and the minimum γ that were smaller than the intrinsic differences between the model and the data. This led to an uncertainty in k_1 and k_2 of ~25%.

Because the isotherm, which depends on k_1 and k_2, was required to generate the loops from which k_1 and k_2 themselves were determined, the process used to find the optimal values that matched the data was necessarily iterative. We began the iteration process by picking an isotherm from the literature (22) and then varying k_1 and k_2 as described above to find the optimum values for a given isotherm. However, our results were sensitive to only the average slope of the isotherm and not to its particular shape.

RESULTS

Equilibrium surface tension. The results of these tests are shown in Fig. 3. The curves for different bulk concentrations of surfactant TA each begin at a relatively high surface tension and then drop to their equilibrium values. The time scale for the drop in surface tension varied with concentration and is on the order of many seconds to minutes. This time scale characterizes the diffusional nature of this static measurement (see DISCUSSION). Figure 3 demonstrates that the equilibrium surface tension changes as the concentration of surfactant TA is changed. These data are used to generate the isotherm relating interfacial concentration of surfactant to surface tension (see below).

Dynamic tests. Figure 4, *A–D*, illustrates typical examples of the loops obtained by plotting γ vs. A for surfactant TA. The data for a variety of bulk concentrations, frequencies, and area ratios clearly demonstrate that, for sufficiently high bulk concentration of surfactant (Fig. 4, *A* and *B*), a minimum surface tension is reached that remains approximately constant as interfacial area decreases, which is consistent with previous observations (10, 24, 28). In some cases, however, a slight upward drift appears in surface tension once the minimum value has been reached (Fig. 4, *B* and *C*). Also apparent are some random fluctuations in surface tension in this region of relatively constant surface tension that may correspond to the "clicking" described by Schürch (22); these are especially obvious at lower frequencies and higher bulk concentrations.

Frequency has several effects on the shape of the loops, which are most apparent at the higher bulk concentrations (Fig. 4, *A–C*). First, as the cycling rate increases, so does the maximum surface tension attained.

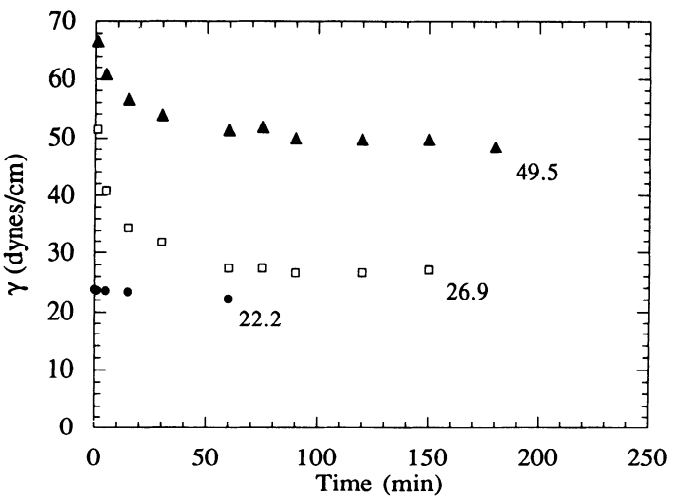

FIG. 3. γ vs. time after forming bubble of radius 0.4 mm. Bulk concentrations (C) are 0.730 mg/ml (●), 0.073 mg/ml (□), and 0.0073 mg/ml (▲). Nos. along each data set, equilibrium γ used at that C.

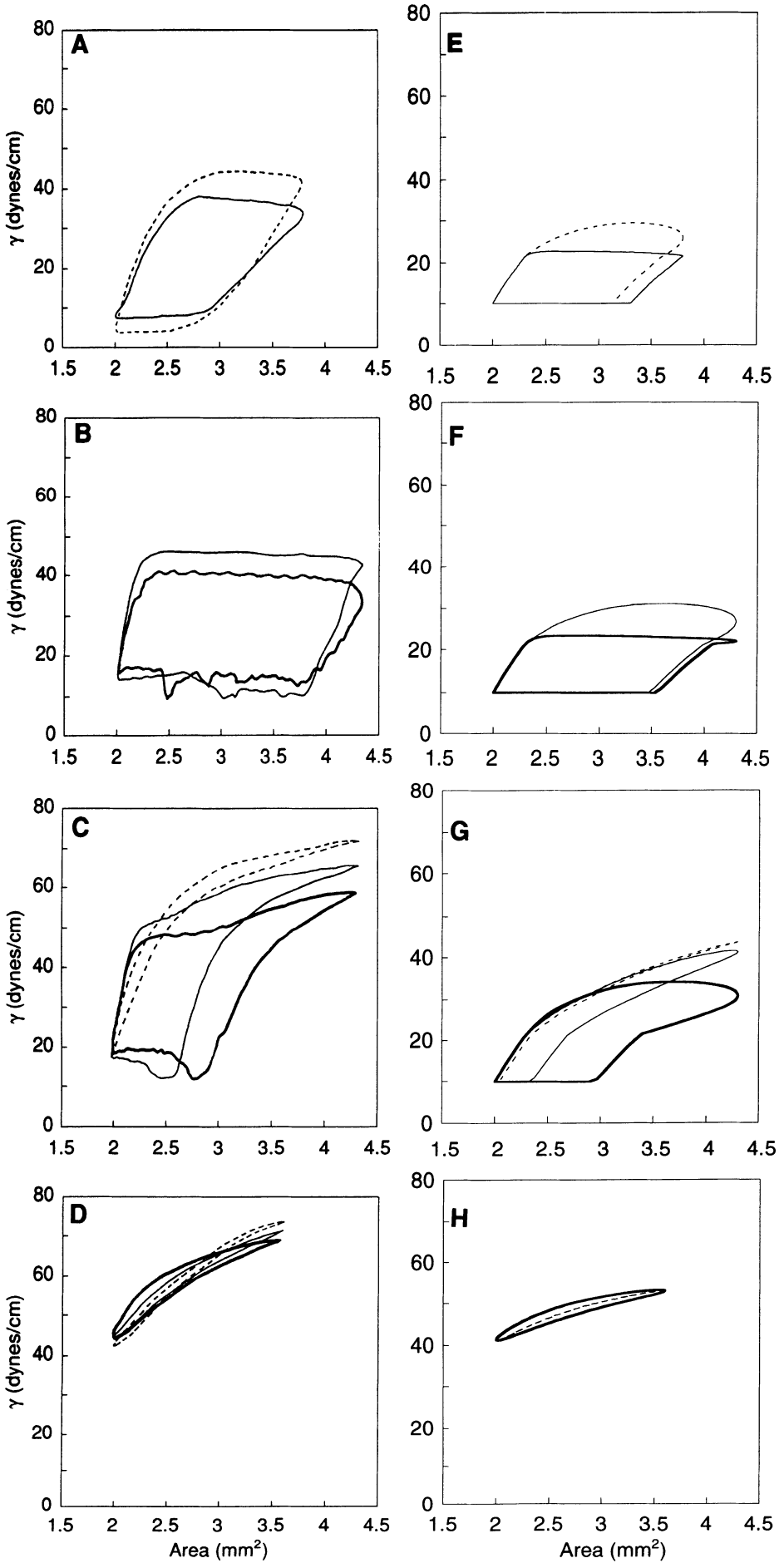

FIG. 4. Stationary-state γ-A loops at frequencies of 1 cycle/min (heavy solid line), 10 cycles/min (light solid line), and 100 cycles/min (dashed line). Shown are experimental results (A–D) and predictions of model with adsorption coefficient k_1 (10^5 $cm^3 \cdot g^{-1} \cdot min^{-1}$) and desorption coefficient k_2 (1 min^{-1}) (E–H). A and E: C = 7.3 mg/ml. B and F: C = 0.73 mg/ml. C and G: C = 0.073 mg/ml. D and H: C = 0.0073 mg/ml. Loop directions are clockwise.

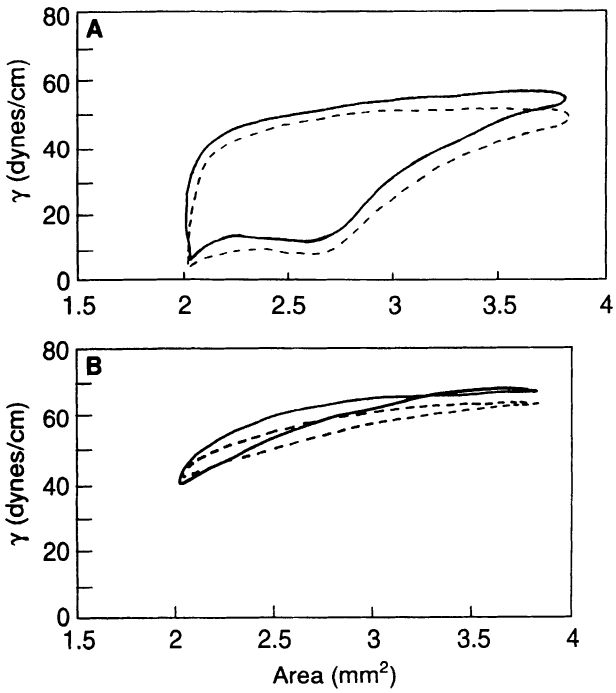

FIG. 5. Stationary-state γ-A loops at frequency of 10 cycles/min for surfactant TA at C = 0.73 mg/ml (A) or C = 0.0073 mg/ml (B) in 5.5 mM $CaCl_2$ (solid line) or normal saline with 5.5 mM $CaCl_2$ (dashed lines).

Second, at lower concentration, the area at which the minimum surface tension is first reached during interfacial compression decreases with increasing cycling rate (Fig. 4C). Third, and perhaps most interesting, is the finding that $\partial\gamma/\partial A$ at the start of surface expansion (i.e., the slope of *segment EF*) is independent of cycling rate and generally exceeds $\partial\gamma/\partial A$ at the early stages of area contraction (slope of *segment CD*). These observations, in part, formed the basis for the model formulation.

Whereas the loops at higher bulk concentrations (Fig. 4, A and B) all exhibited a plateau of minimum surface tension consistent with monolayer collapse and considerable hysteresis, this behavior was not apparent at the lowest concentration examined (Fig. 4D). Instead, there was little hysteresis and the lowest surface tension, which occurred at the minimum interfacial area only, was higher than that observed at higher bulk concentrations. There was also relatively little frequency dependence in the low concentration result.

No significant difference was found between loops whether saline (with 5 mM $CaCl_2$) or 5 mM $CaCl_2$ alone was used to dilute the surfactant in the bulk phase (Fig. 5), which is in agreement with the results of other investigators (9).

Theoretical results. The results from the model can be cast in terms of two governing dimensionless parameters, k_2/k_1C, the relative importance of desorption to adsorption, and k_1C/ω, the adsorption time scale relative to cycle time. In presenting the results, it is useful (although not necessary) to introduce a third parameter, k_2/ω (desorption time scale relative to cycle time). Figure 6A shows the stationary-state loops predicted by the model of surface tension as a function of area for varying values of the parameter k_2/k_1C while holding k_1C/ω at a relatively low value. Increasing k_2/k_1C causes a concomitant increase in the lowest surface tension during a cycle. Figure 6B shows the stationary-state loops for varying values of the parameter k_1C/ω while holding k_2/ω at a relatively low value. Increasing k_1C/ω leads to greater hysteresis in the loops; as in the experimental data (Fig. 4, A–D), the hysteresis is largest for the smallest frequency and the largest bulk concentration.

The model predictions were compared with experimental data. Data at a low concentration (Fig. 4D) were used to determine the value of k_2/k_1C by using figures like Fig. 6A. Data at the higher bulk concentrations (which are relatively insensitive to the value of k_2) were used to determine k_1C/ω (in the fashion shown in Fig. 6B). Comparison of the model results with the experimental data yields $k_1 = 10^5\ cm^3 \cdot g^{-1} \cdot min^{-1}$ and $k_2 = 1\ min^{-1}$ for surfactant TA.

Figure 4, E–H, shows predictions of the model for surface tension with these best estimates for k_1 and k_2 using the isotherm (solid line) shown in Fig. 2. The model is able to correctly describe most of the features shown in the experimental loops. First, the model correctly predicts the overall shape of the loops and the changes in loop shape with bulk concentration (although the model underpredicts the maximum surface tension for all loops). The model also mimics the experimental observation that $\partial\gamma/\partial A$ at the start of surface expansion (i.e., the slope of *segment EF*) is independent of cycling rate and exceeds $\partial\gamma/\partial A$ during the early stages of area contraction. This follows directly from the model formulation because each cycle begins at *point E* with the same surface tension and interfacial area, and because desorption does not occur until surface tension is higher than the

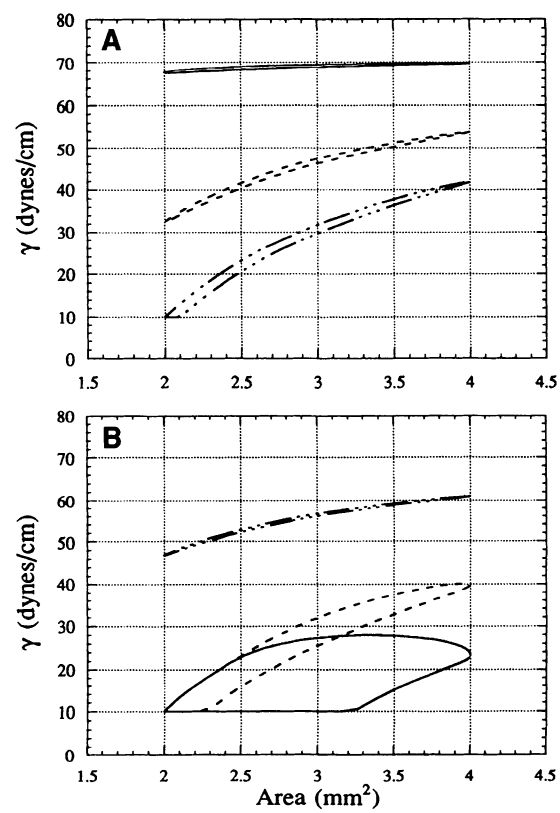

FIG. 6. γ-A loops obtained from computational model. A: k_1C/ω = 0.2 (where ω is oscillation frequency). k_2/k_1C = 0.1, 1.0, and 10 and correspond to dot-dashed, dashed, and solid lines, respectively. B: k_2/ω = 0.2. k_1C/ω = 0.1, 1.0, and 10 and correspond to dot-dashed, dashed, and solid lines, respectively.

minimum equilibrium value, the cycling frequency will have no effect until the first regime is reached.

The model also correctly predicts that for the lower bulk concentrations (Fig. 4, *G* and *H*) hysteresis in the loops is decreased and no longer is a plateau region of constant surface tension achieved (Fig. 4*H*). k_2 was most important for demonstrating the latter behavior. The model further correctly predicted that at lower bulk concentrations (Fig. 4*G*) the area at which the minimum surface tension is reached decreases as frequency increases. This phenomenon is controlled by the parameter k_1C/ω and thus is not seen for the higher bulk concentrations.

The result for the minimum surface tension achieved on the plateau for the higher bulk concentrations was qualitatively correct, but the actual minimum surface tension achieved was different from one experiment to another. Because the model uses a single isotherm to characterize all of the loops, this behavior could not be recovered.

Isotherm relating interfacial surfactant concentration to surface tension. The iterative procedure of finding an isotherm and then determining k_1 and k_2 yielded the values for the parameters given above and the isotherm shown in Fig. 2. Also shown on Fig. 2 is a second isotherm found using data from the inflation phase of one of the high-frequency loops. Substantial differences between these two isotherms are apparent. A possible explanation for this difference is given in DISCUSSION.

DISCUSSION

This study has involved an examination of the dynamic behavior of surfactant TA under a variety of frequencies at differing bulk concentrations. Using a simple analytic model that accounts for surfactant dynamic adsorption and desorption and for squeeze-out, we can generate loops of surface tension as a function of interfacial area that show good agreement with dynamic data from a bubble surfactometer.

Many experimental investigations have been conducted to determine the effects of dynamic compression on surface tension of lung surfactants and their analogues (e.g., Refs. 6, 14, 20, 23, 25, 28). However, no model was proposed in these studies to explain the mechanism for the dynamic changes in surface tension observed. In our studies, we used a theoretical model to analyze similar data, under a variety of experimental conditions, with the goal of better understanding the process by which surfactant molecules enter and leave the interface.

We modeled surfactant TA as a single component entering and leaving the interface as a function of interfacial surfactant concentration. Surfactant TA has several constituents, however, and there is surely differential squeeze-out of these different components (3, 10). In addition, there may be interactions between the different species that affect adsorption and desorption during this cyclic process. Nonetheless, this simple model gives good agreement with the experimental data, suggesting that the most important and relevant processes are captured by this simulation.

Modeling of the conditions for surfactant adsorption and desorption at the interface led us to adopt several assumptions to optimize the fit to the experimental data. These assumptions include *1*) there exists a maximum surfactant concentration to which the interface can be dynamically packed, and when interfacial area is reduced from this point, surfactant is squeezed out from the surface; *2*) transport of surfactant to the interface is adsorption rather than diffusion limited; *3*) when the interfacial concentration of surfactant is less than its maximum equilibrium value (Γ^*), adsorption and desorption are controlled by Langmuir kinetics; and *4*) for interfacial surfactant concentrations between the maximum equilibrium value and the maximum packing concentration, the surfactant is "frozen" in the surface and can neither adsorb nor desorb. Support for each of these assumptions and/or findings is given below.

The experimental data clearly demonstrate that, when the interfacial film is compressed beyond a certain point, surface tension remains nearly constant as interfacial area is further reduced (high film compressibility) (10). Tchoreloff et al. (28) found a similar result for lung surfactant extract, attributing the phenomenon to squeeze-out of the interfacial material that they quantified by measuring the changes in loop shape for the first few cyclic compressions (using a Langmuir-type film balance). Furthermore, using a Langmuir-Blodgett technique, they demonstrated that following this squeeze-out a sublayer of surfactant is formed just beneath the interface.

In this study we assumed that the transport of surfactant molecules to the interface is adsorption limited. In fact, a diffusional boundary layer of thickness $(D/\omega)^{1/2}$ (where D is the surfactant bulk diffusion coefficient) will develop at the interface. Transport through this boundary layer is complex, involving unsteady transport, micellar formation and diffusion, and solubility limitations (13). Whereas further studies will be necessary to characterize transport though this boundary layer, the success of our adsorption-limited model in describing the frequency dependence and bulk concentration dependence of the γ-A loops suggests that the process is not diffusion limited.

We believe the loops generated during cycling are adsorption limited because of the material that is squeezed out of the interface (28) during compression of this layer. This depot of surfactant just below the interface may be supplying molecules to the surface during adsorption and receiving surfactant during squeeze-out. Thus, after a transient equilibration period (the length of which would be diffusion limited) during which this subsurface layer is formed, there would be no diffusive barrier to adsorption because all of the molecules are immediately available to the interface. Our current model does not yet explicitly account for this subsurface depot of surfactant other than our assumption that there does not exist a diffusive barrier to adsorption. This is also consistent with our assumption that in the third regime during squeeze-out the surfactant lost from the interface is immediately well mixed with the bulk.

It should be noted here that we are emphasizing the time scale controlling adsorption during cyclic volume changes. The time scale for adsorption in our dynamic model varies as $1/k_1C$ (see *Eq. 1*). For measurements of surface tension in which a fixed interfacial area is created and then surface tension monitored as a function of time, one would expect transient diffusional time scales to be much more important because molecules must be

brought from the bulk to first saturate the interface. In this case, the time scale would vary as $(\Gamma_{eq}/C)^2/D$ (12). This is borne out by the data in Fig. 3, which shows time scales on the order of many minutes for saturation of the interface, and is further substantiated by data from other investigators (23) demonstrating that the equilibration time scales roughly as $1/C^2$.

The third and fourth assumptions are related, as these describe the nature of the adsorption and desorption processes. For interfacial concentrations less than the maximum equilibrium value, we assume that the dynamics of adsorption and desorption are controlled by *Eq. 1*. This is the simplest dynamic equation consistent with the Langmuir isotherm (2). We have assumed here that k_1 and k_2 are not a function of bulk or interfacial surfactant concentration. There is, in fact, data to the contrary showing that k_2 decreases as the interfacial concentration of surfactant increases (27). We made the simplifying assumption that k_1 and k_2 are constant below the maximum equilibrium interfacial concentration, whereas above this concentration they drop to zero. This is obviously a coarse approximation, but as it seems to describe the available data reasonably well, it would be difficult to justify a more complicated adsorptive-desorptive model.

Goerke and Clements (7) add support to this approximation when they point out that for surface tension >25 dyn/cm interfacial relaxation toward equilibrium occurs very rapidly (in s), whereas for surface tension lower than this the relaxation process is very slow (in h); they add that spontaneous adsorption occurs only for surface tension >25 dyn/cm. In addition, Smith and Stamenovic (26) performed experiments on excised canine lungs comparing pressure-volume curves from lobes with constant-surface tension liquids lining the air spaces with those obtained from normal lobes. The results from stepwise expiration and inspiration indicate that sorption occurs much more rapidly when surface tension of the lining layer is above the equilibrium value (~28 dyn/cm) than when it is below this value.

The experimental results and the results from matching our model to these data led to a number of conclusions. First, as noted by other investigators (10, 24, 28), there is a nonzero minimum surface tension that is not lowered on further compression of the surface (within the range of compressions considered in these experiments). This observation is attributable to a phase change of the surface film from the liquid-condensed state to a solid state (28), and as the interfacial area of the surface is further lowered, squeeze-out of surfactant results. Notably, this phenomenon was not seen for a surfactant concentration of 0.0073 mg/ml. From our model, we find that for a concentration higher than ~0.030 mg/ml there is a balance over each cycle between adsorption [$k_1C(\Gamma^* - \Gamma)$ in *Eq. 1*] and squeeze-out; however, for bulk concentrations below this value we find the balance now exists between adsorption and desorption ($k_2\Gamma$ in *Eq. 1*).

The model effectively described the shape of the γ-A loops, showing the largest hysteresis at the smallest frequencies and the largest bulk concentrations. The model successfully predicts the sharp increase in surface tension that occurs on reinflation (*segment EF*). Notably, we did not have to assume during the early stages of expansion any lack of respreading (17, 28) of the surfactant or cracking apart to form condensed "ice floes" and stretches of "open sea" (7). Instead, the sharp increase in surface tension was found to be a consequence of squeeze-out, decreasing the available surfactant, and the steep increase in surface area A that occurs at the low interfacial areas at which inflation begins.

One of the very important experimental observations of our study was the lack of frequency dependence exhibited by the rate of increase in surface tension early in expansion (*segment EF*). To our knowledge, this phenomenon has not been reported by other investigators. One would expect that when interfacial concentration is maximum (along and near *segment DE*) viscous effects in the interface, proportional to the product of surface viscosity (8) and frequency, would be most apparent. Because this was not seen experimentally, it follows that surface viscosity is unlikely to play a significant role in the dynamics of the surfactant TA.[1] Our model indicates that this frequency-independent behavior follows directly from the assumption of an insoluble monolayer (neither adsorbing nor desorbing) for interfacial concentrations greater than Γ^* but less than Γ_{max}: if adsorption started at the onset of expansion (*point E*), then the slope of *segment EF* would increase with decreasing frequency.

A weakness in the analytic model was found on closer examination of the isotherm relating surface tension to surfactant interfacial concentration. Whereas the distribution of surfactant in the air-liquid interface should become uniform during deflation, substantial inhomogeneities may develop during inflation because of cracking of the surfactant layer and the formation of islands of surfactant material on the interface (7); this may significantly affect the relationship between interfacial surfactant concentration and surface tension in this nonequilibrium state. As discussed in MATERIALS AND METHODS and in RESULTS, two different techniques were used to determine the isotherm; the first, using the result from the equilibrium surface tension measurements and dynamic data from the deflation phase of the loops, assumes that the surfactant is uniformly spread in the interface; the second technique, assuming that negligible amounts of surfactant enter or leave the interface during inflation at higher frequency, does not require such an assumption.

As shown in Fig. 2, for $\Gamma < \Gamma^*$, we found that the two techniques described for determining the isotherm gave different results. This suggests that whereas squeeze out plays an important role in determining surfactant hysteresis, cracking of the surfactant layer may also be a major contributor to the hysteresis. Although the evidence is indirect, this is the likely explanation for the underprediction by the model of the maximum surface tension reached in all of the experimental loops.

[1] Hall et al. (8) showed that the effects of dilatational surface viscosity are strictly zero when the bubble is at minimum radius (*point E*). However, because the surface viscosity itself (assumed constant by Hall et al.) is maximal in the neighborhood of *point E* and because no frequency dependence is seen along *segment EF* (nor, for that matter, along *segment DE*), this suggests that because the effects of surface viscosity are not manifest in these regions they are unlikely to have significant effects elsewhere in the cycle. Edwards et al. (4) commented on the difficulty of distinguishing dilatational viscosity from compositional elastic effects without a surfactant transport model like that described in the present work.

One potential artifact of the experiments is the loss of surfactant by leakage into the attached tube that pierces the bubble. If the tube is an escape route, then surfactant may be lost when the film is highly compressed and the measured surface tension would be higher than if the bubble were completely isolated. No provision in our model was made to account for this phenomenon. However, because our measurements were made at a periodic stationary state and *1*) there did not appear to be greater discrepancies between the experimental data and the model at the different frequencies and *2*) the experimental data were relatively rate independent along the minimum surface tension plateau (*segment DE*), leakage does not appear to have a significant role unless it occurred on a time scale much less than that corresponding to our maximum cycling rate.

Previous studies have characterized lung surfactant and their analogues in terms of the rate of adsorption of surfactant to a static constant-area interface (6, 16, 18, 23). Although this provides valuable information on how long it will take for the surfactant to first be adsorbed into an interface (which may be critical in the delivery of surfactant to preterm infants with RDS), it fails to describe the periodic and dynamic process that a surfactant undergoes during normal breathing. Our model suggests that the dynamic properties of natural and artificial lung surfactants can be characterized in terms of three properties: *1*) the isotherm relating interfacial concentration (Γ) to surface tension, *2*) dynamic adsorption rate (k_1), and *3*) dynamic desorption rate (k_2).

γ_{min} and γ^* have been determined for a wide variety of lung surfactants and their analogues. However, k_1 and k_2 are new parameters that have not been characterized for other lung surfactant preparations. These parameters are very important for determining the rate of increase in surface tension on reinflation, loop hysteresis, and extent of squeeze-out. Slama et al. (25) and Notter et al. (17) have suggested that these lung surfactant characteristics might also be important for normal lung functions including alveolar recruitment and uniform ventilation. Characterization of these dynamic parameters may lead to better artificial surfactant preparations for the treatment of RDS.

This work was supported by National Heart, Lung, and Blood Institute Grants HL-33009, HL-45679, HL-763307, HL-33003 and grants from the Whitaker Foundation and the Freeman Foundation.

Address for reprint requests: M. Johnson, Rm. 3-264, MIT, 77 Massachusetts Ave., Cambridge, MA 02139.

Received 12 October 1993; accepted in final form 1 August 1994.

REFERENCES

1. **Borwankar, R. P., and D. T. Wasan.** The kinetics of adsorption of surface active agents at gas-liquid surfaces. *Chem. Eng. Sci.* 38: 1637–1649, 1983.
2. **Chang, C. H., and E. I. Franses.** Modified Langmuir-Hinshelwood kinetics for dynamic adsorption of surfactants at the air/water interface. *Colloids Surf.* 69: 189–201, 1992.
3. **Chung, J. B., R. E. Hannemann, and E. I. Franses.** Surface analysis of lipid layers at air/water interfaces. *Langmuir* 6: 1647–1655, 1990.
4. **Edwards, D. A., H. Brenner, and D. T. Wasan.** *Interfacial Transport Processes and Rheology*. Boston, MA: Butterworth-Heinemann, 1991, chapt. 8.
5. **Enhorning, G.** Pulsating bubble technique for evaluating pulmonary surfactant. *J. Appl. Physiol.* 43: 198–203, 1977.
6. **Fuchimukai, T., T. Fujiwara, A. Takahashi, and G. Enhorning.** Artificial pulmonary surfactant inhibited by proteins. *J. Appl. Physiol.* 62: 429–437, 1987.
7. **Goerke, J., and J. A. Clements.** Alveolar surface tension and lung surfactant. In: *Handbook of Physiology. The Respiratory System. Mechanics of Breathing*. Bethesda, MD: Am. Physiol. Soc., 1986, sect. 3, vol. III, pt. 1, chapt. 16, p. 247–262.
8. **Hall, S. B., M. S. Bermel, Y. T. Ko, J. Palmer, G. Enhorning, and R. H. Notter.** Approximations in the measurement of surface tension on the oscillating bubble surfactometer. *J. Appl. Physiol.* 75: 468–477, 1993.
9. **Hardy, P., A. Lysikiewicz, and G. Enhorning.** Hypophase effect on a DPPC monolayer. *Prog. Respir. Res.* 18: 10–17, 1984.
10. **Hildebran, J. N., J. Goerke, and J. A. Clements.** Pulmonary surface film stability and composition. *J. Appl. Physiol.* 47: 604–611, 1979.
11. **Horn, L. W., and S. H. Davis.** Apparent surface tension hysteresis of a dynamical system. *J. Colloid Interface Sci.* 51, *Suppl.* 3: 459–476, 1975.
12. **Jiang, Q., and Y. C. Chiew.** A simple test for diffusion-controlled adsorption at an air/water interface. *Langmuir* 9: 273–277, 1993.
13. **Johannsen, E. C., J. B. Chung, C. H. Chang, and E. I. Franses.** Lipid transport to air/water interfaces. *Colloids Surf.* 53: 117–134, 1991.
14. **Keough, K. M., C. S. Parson, P. T. Phang, and M. G. Tweeddale.** Interactions between plasma proteins and pulmonary surfactant: surface balance studies. *Can. J. Physiol. Pharmacol.* 66: 1166–1173, 1988.
15. **King, R. J., and J. A. Clements.** Surface active materials from dogs lung. I. Method of isolation. *Am. J. Physiol.* 223: 707–714, 1972.
16. **King, R. J., and J. A. Clements.** Surface active materials from dogs lung. II. Composition and physiological correlations. *Am. J. Physiol.* 223: 715–726, 1972.
17. **Notter, R. H., R. Taubold, and R. D. Mabis.** Hysteresis in saturated phospholipid films and its potential relevance for lung surfactant function in vivo. *Exp. Lung Res.* 3: 109–127, 1982.
18. **Pérez-Gil, J., J. Tucker, G. Simatos, and K. M. Keough.** Interfacial adsorption of simple lipid mixtures combined with hydrophobic surfactant protein from pig lung. *Biochem. Cell Biol.* 70: 332–338, 1992.
19. **Possmayer, F., W. Yu, and M. Weber.** Calcium-protein-lipid interactions in pulmonary surfactant. *Prog. Respir. Res.* 18: 112–120, 1984.
20. **Rana, F. R., A. J. Mautone, and R. A. Dluhy.** Surface chemistry of binary mixtures of phospholipids in monolayers. Infrared studies of surface composition at varying surface pressures in a pulmonary surfactant model system. *Biochemistry* 32: 3169–3177, 1993.
21. **Scarpelli, E. M.** *Surfactants and the Lining of the Lung*. Baltimore, MD: John Hopkins Univ. Press, 1988.
22. **Schürch, S., H. Bachofen, J. Goerke, and F. Possmayer.** A captive bubble method reproduces the in situ behavior of lung surfactant monolayers. *J. Appl. Physiol.* 67: 2389–2396, 1989.
23. **Schürch, S., F. Possmayer, S. Cheng, and A. M. Cockshutt.** Pulmonary SP-A enhances and appears to induce surface sorting of lipid extract surfactant. *Am. J. Physiol.* 263 (*Lung Cell. Mol. Physiol.* 7): L210–L218, 1992.
24. **Seeger, W., G. Stöhr, H. R. D. Wolf, and H. Neuhof.** Alteration of surfactant function due to protein leakage: special interaction with fibrin monomer. *J. Appl. Physiol.* 58: 326–338, 1985.
25. **Slama, H., W. Schoedel, and E. Hansen.** Lung surfactant: film kinetics at the surface of an air bubble during prolonged oscillation of its volume. *Respir. Physiol.* 19: 233–243, 1973.
26. **Smith, J. C., and D. Stamenovic.** Surface forces in lungs. I. Alveolar surface tension-lung volume relationships. *J. Appl. Physiol.* 60: 1341–135, 1986.
27. **Tabak, S. A., R. H. Notter, J. S. Ultman, and S. M. Dinh.** Relaxation effects in the surface pressure behavior of dipalmitoyl lecithin. *J. Colloid Interface Sci.* 60: 117–125, 1977.
28. **Tchoreloff, P., A. Gulik, B. Denizot, J. E. Proust, and F. Puisieux.** A structural study of interfacial phospholipid and lung surfactant layers by transmission electron microscopy after Blodgett sampling: influence of surface pressure and temperature. *Chem. Phys. Lipids* 59: 151–165, 1991.
29. **Weibel, E. R.** *The Pathway for Oxygen*. Cambridge, MA: Harvard Univ. Press, 1984.